Evolution of the Internal Dynamics of Two Globular Proteins from Dry Powder to Solution

Javier Pérez,* Jean-Marc Zanotti,# and Dominique Durand*,#
*LURE, CNRS-MENESR-CEA, Centre Universitaire Paris-Sud, B.P. 34, F-91898 Orsay Cedex, and #LLB, CEA-CNRS, CEA Saclay, F-91191 Gif-sur-Yvette Cedex, France

ABSTRACT Myoglobin and lysozyme picosecond internal dynamics in solution is compared to that in hydrated powders by quasielastic incoherent neutron scattering. This technique is sensitive to the motions of the nonexchangeable hydrogen atoms in a sample. Because these are homogeneously distributed throughout the protein structure, the average dynamics of the protein is described. We first propose an original data treatment to deal with the protein global motions in the case of solution samples. The validity of this treatment is checked by comparison with classical measurements of the diffusion constants. The evolution with the scattering vector of the width and relative contribution of the quasielastic component was then used to derive information on the amount of local diffusive motions and their characteristic average relaxation time. From dry powder to coverage by one water layer, the surface side chains progressively acquire the possibility to diffuse locally. On subsequent hydration, the main effect of water is to improve the rate of these diffusive motions. Motions with higher average amplitude occur in solution, about three times more than for a hydrated powder at complete coverage, with a shorter average relaxation time, ~4.5 ps compared to 9.4 ps for one water monolayer.

INTRODUCTION

The extreme efficiency and specificity of the functions of proteins is the consequence of their specific three-dimensional fold and their ability to react to the environment by adapting their structure. This adaptability supposes intrinsic flexibility and dynamics (McCammon and Harvey, 1987). Protein dynamics is an intrinsic property of each protein, as is its structure, and may depend on external parameters that are not specifically related to its particular function. Among these parameters, temperature and hydration in particular have been investigated in the past few years.

Hydration is known to strongly influence protein dynamics and activity. Many experiments have been performed on protein powders at different levels of hydration, showing that water acts as a "plasticizer" of the protein conformation by reestablishing the dynamic properties of proteins (for a review, see Gregory, 1995). From the point of view of function, one of the most striking effects of water influence is certainly the onset of activity of several enzymes around 0.2 g water/g dry protein (denoted as 0.2 g/g) (Drapron, 1985; Rupley and Careri, 1991), whereas they remain inactive at lower levels of hydration. The effect of hydration has been exhaustively studied in the case of a small enzyme, hen egg white lysozyme (Rupley et al., 1983). For example, it is interesting to know that the full hydration of lysozyme by water occurs at 0.38 g/g, if this is defined as the hydration level above which the specific heat capacity of the protein remains constant (Yang and Rupley, 1979). A second definition of complete hydration is sometimes used, the hydration level below which no ice formation occurs, and gives a slightly lower value of 0.34 g/g (Kuntz and Kauzmann, 1974). The onset of activity thus occurs well before the protein is completely hydrated.

The crucial influence of water on protein dynamics has also been shown in the hydration dependence of the so-called protein dynamical transition temperature. This transition is characterized by the appearance of protein internal diffusive motions, whereas only spatially restricted harmonic vibrations would be allowed at lower temperatures (Knapp et al., 1982; Doster et al., 1989; Ferrand et al., 1993). Interestingly, the transition temperature seems to remain around 200 K for many hydrated proteins, suggesting that the phenomenon is due to very basic characteristics of protein structure. However, dry proteins do not show this transition. Rayleigh scattering of Mössbauer radiation experiments have demonstrated that met-myoglobin mean-square atomic fluctuations are a (harmonic) linear function of temperature in the case of a dry sample, at least up to 300 K (Goldanskii and Krupyanskii, 1989). The same conclusions were drawn in the case of bacteriorhodopsin (Ferrand et al., 1993). A profound investigation of the effect of hydration on the dynamical transition was carried out by Gregory and Chai (1993). They suggest, based on positron and positronium lifetime measurements in lysozyme, that the same kind of transition occurs at higher temperatures at decreased hydration levels, bringing, for example, a temperature transition of 298 K at 0.12 g/g hydration. In any case, the plasticizing effect of water is clearly pointed out in these experiments, the hydrogen bonds involving water molecules probably offering energetical pathways between different residue side-chain conformations.

Received for publication 20 November 1998 and in final form 22 April 1999.

Address reprint requests to Dr. Javier Pérez, LURE, CNRS-MENESR-CEA, Centre Universitaire Paris-Sud, Bât. 209D, B.P. 34, F-91898 Orsay Cedex, France. Tel.: 33-1-64-46-88-20; Fax: 33-1-64-46-88-20; E-mail: perez@lure.u-psud.fr.

0006-3495/99/07/454/16 $2.00

A striking consequence of the dynamical transition is the advent of protein function at the same time as anharmonic motions, as has been shown in the case of bacteriorhodopsin (Ferrand et al., 1993) and ribonuclease A (Rasmussen et al., 1992). This concomittance, together with the role of water mentioned above, clearly shows the strong relation between hydration, anharmonic dynamics, and biological activity. The aim of the present work is precisely to investigate the relation between protein hydration and anharmonic dynamics from dry and hydrated powders to solution. As stated before, hydrated powders are biologically relevant model systems in the sense that the protein is active. But this situation implies multiple protein-protein interactions, which do not exist in the physiological medium and may limit the conformational flexibility of each protein. Yang and Rupley (1979) have shown that the heat capacity of a lysozyme water system does not change above 0.38 g/g of hydration, but these are not direct measurements of the dynamics and do not prove that the dynamical properties remain unchanged. Indeed, if protein activity might exist in hydrated powders, it is still less efficient than in solution, as was measured by Rupley et al. (1980, 1983). Our interest here is to see, by incoherent quasielastic neutron scattering (IQENS), the point to which certain protein internal dynamic characteristics are modified in solution with respect to a hydrated powder.

IQENS is a technique sensitive mainly to nonexchangeable hydrogen diffusive motions, and, in principle, it provides relaxation times and motion shapes at the molecular level. As a result, it directly measures the average protein dynamics. In the past few years, many IQENS studies have been carried out on water dynamics at the surface of perdeuterated C-phycocyanin (Bellissent-Funel et al., 1996), bacteriorhodopsin (Lechner et al., 1994a, b), and myoglobin (Settles and Doster, 1996) and on the dynamics of the proteins themselves as a function of hydration (Fitter et al., 1996, 1997; Diehl et al., 1997; Zanotti et al., 1997) or as a function of denaturant concentration (Receveur et al., 1997). The range of time scales at which dynamical events occur in a protein is very wide, from 10^{-15} s to a few seconds, because of the high variety of intramolecular interactions. Of this enormous spectral range, however, each experimental technique is only able to exploit a narrow window, with a corresponding type of motion. In particular, the rotational correlation time of protein surface water, which has been shown by ^{17}O spin relaxation dispersion to be ~20 ps for a globular protein (Denisov and Halle, 1995), fall in a time scale (10^{-13} to 10^{-9} s) that is readily accessible by IQENS. The dynamics of protein surface residues, which strongly couples with water dynamics, fall in the same time scale (Kneller and Smith, 1994).

So far, most of the IQENS studies concerning the dynamics of water-soluble globular proteins have been performed on protein powders. There is a strong temptation to experiment with IQENS on protein solutions, which is still a challenge for neutron scattering. The difficulty with this arises from the high amount of unwanted solvent scattering, which is nearly suppressed in the case of a hydrated powder, and from protein diffusion in solution, which creates an extra Doppler effect on neutron scattering and has to be correctly evaluated and deconvoluted.

In this work we have taken up this challenge and performed a comparative study on picosecond dynamics of a protein solution and corresponding hydrated powders at two or three levels of hydration. Beyond the interest of the influence of water on protein dynamics, the mere fact of being able to work with solutions would allow better comparisons with the results from other techniques.

MATERIALS AND METHODS

Samples

Salt-free lyophilized horse heart myoglobin (17.4 kDa) and hen egg white lysozyme (14.3 kDa) were purchased from Sigma and ICN, respectively. The proteins were first dissolved in pure D_2O at a concentration of ~6 mM, then extensively dialyzed against D_2O, to exchange labile hydrogen atoms. After removing aggregates by centrifugation (10 min at 10,000 × *g*), the samples were lyophilized. The hydrated powders were obtained by rehydrating the lyophilized material by vapor phase adsorption of D_2O. The water content of the samples was determined by weighing. The hydrated powder samples, each containing ~150 mg of dry protein, were sealed in a thin-walled aluminum cell of 50-mm diameter and 1.3-mm interval spacing. The solution samples were obtained by dissolution of the D_2O-exchanged lyophilized protein in pure D_2O, at a protein concentration of ~60 g/liter. We measured a pH of 4.25 and 7.45 for lysozyme and myoglobin solutions, respectively. From the theoretical charged side-chain pKa's (Riès-Kautt and Ducruix, 1997), the net charge is +13.5 for lysozyme and 0 for myoglobin. The solutions were kept in the same type of cell as the powder samples.

Neutron measurements

The experiments were performed with the time-of-flight (TOF) spectrometer IN6 (ILL, Grenoble), using neutrons of 5.12-Å wavelength. The scattering was measured over a wavevector range of $0.3 < Q < 2.0$ Å^{-1} at room temperature. All samples, including the vanadium standard and the empty aluminum can, were oriented at 135° with respect to the incident beam. At 5.12-Å wavelength, this orientation allows the collection of data over the whole range of detectors. However, the absorption is very high at high angles for the solution samples, for which the last high Q values have been suppressed from our analysis. The measured TOF spectra were normalized using the vanadium standard, corrected for transmission and geometry effects, and transformed into energy transfer spectra by the "inx" routine from ILL. No correction for multiple scattering has been performed, because the lowest transmission obtained with the solution samples is 90%. To improve the statistics, the spectra derived from the 235 detectors of IN6 were binned into 18 constant angle spectra, with Q_0 ranging from 0.49 to 2.04 Å^{-1}. The resulting data were analyzed with the program Agathe by Marc Bée (ILL).

Incoherent neutron scattering

An exhaustive description of quasielastic neutron scattering can be found in Bée (1988). The application to protein dynamics was reviewed by Smith (1991). Here we recall some useful basic notions. A neutron scattering experiment consists of irradiating a sample by a parallel, usually monochromatic beam of incident neutrons. The incident beam is characterized by a wavevector, $\mathbf{k}_0$, and an energy, $E_0 = \hbar\omega_0$, which are related by the equation $\hbar\omega_0 = \hbar^2 k_0^2/(2m)$, where $\hbar$ is the Planck constant divided by 2π and m is the neutron mass. The incident neutrons exchange momentum and

energy with the sample scatterers. The energy transfer, $\hbar\omega$, is given by $\hbar\omega = \hbar^2/2m(k^2 - k_0^2)$, where $\hbar^2k^2/2m$ is the final energy of the scattered neutron. The scattering vector, $\mathbf{Q}$, is defined as $\mathbf{Q} = \mathbf{k}_0 - \mathbf{k}$, where $\mathbf{k}$ is the wavevector of the scattered neutron. In the case where there is no energy transfer between the sample and the incident neutron ($\hbar\omega = 0$), the scattering vector is termed $\mathbf{Q}_0$, and its amplitude is related to the scattering angle, θ, by the equation $Q_0 = 4\pi \cdot \sin(\theta/2)/\lambda_0$, where $\lambda_0 = 2\pi/k_0$ is the incident wavelength.

Neutrons interact with matter via the atomic nuclei, and because the spin state of these nuclei is undetermined, two kinds of scattering processes take place, coherent and incoherent. Coherent scattering is the product of interference between waves scattered by different atoms, as, for example, in x-ray scattering by electrons. In contrast, incoherent scattering depends only on the correlations between the positions of the same atom at different times. Each of these scattering processes is characterized, for each atomic species, by a scattering length b_{coh} for coherent scattering and b_{inc} for incoherent scattering, the square of the magnitude of which specifies the respective scattering cross sections. The most important feature concerning the magnitudes of b's, from the point of view of our samples, is the very high value of the incoherent cross section of hydrogen, 79.9 barns, as compared to any of the other atomic species in proteins, and especially as compared to that of deuterium, 2.0 barns. This property is the basis of all neutron incoherent scattering on protein samples, that is, atoms other than hydrogens remain almost invisible in the scattering process. As the hydrogen distribution within a protein is almost homogeneous (the amount of exchanged protons replaced by deuterons in the case of D_2O hydration is only a small fraction of total hydrogens), a neutron incoherent scattering experiment reflects the average dynamics of the protein, within a time window related to the experimental conditions.

In an inelastic neutron scattering experiment, the measured quantity is the number of neutrons scattered by the sample at ($\mathbf{Q}$, ω) into a solid angle element $\delta\Omega$ and an energy range $\delta\omega$. The incoherent part of this quantity is directly proportional to the differential cross section,

$$\frac{\partial^2\sigma}{\partial\Omega\,\partial\omega}(\mathbf{Q}, \omega) = \frac{1}{4\pi}\frac{|k|}{|k_0|}\sigma_{inc}S_{inc}(\mathbf{Q}, \omega) \quad (1)$$

where $\sigma_{inc} = 4\pi b_{inc}^2$, $S_{inc}(\mathbf{Q}, \omega)$ is the incoherent scattering function, and the other variables are defined as above. We shall see, at the end of the Data Analysis section, how to handle the small contribution of coherent scattering. Until then, we shall consider it as negligible. In practice, on a TOF spectrometer, the energy of a scattered neutron is calculated from the time taken by the neutron to reach a detector placed at a scattering angle θ. A series of detectors disposed within a wide angular range make it possible to numerically reconstruct $\partial^2\sigma/\partial\Omega\,\partial\omega$ ($\mathbf{Q}$, ω) from $\partial^2\sigma/\partial\Omega\,\partial\omega$ (θ, ω).

The relation between $S_{inc}(\mathbf{Q}, \omega)$ and real space dynamics can be derived through the formalism developed by van Hove (1954). $S_{inc}(\mathbf{Q}, \omega)$ is expressed as the double Fourier transform of the van Hove self-correlation function, $G_s(\mathbf{r}, t)$:

$$S_{inc}(\mathbf{Q}, \omega) = \frac{1}{2\pi}\int G_s(\mathbf{r}, t)e^{i(\mathbf{Q}\cdot\mathbf{r}-\omega t)}d\mathbf{r}\,dt \quad (2)$$

In the classical approximation, $G_s(\mathbf{r}, t)$ represents the probability that any particle is moved by $\mathbf{r}$ within time t and is given by

$$G_s(\mathbf{r}, t) = \frac{1}{N}\sum_{n=1}^{N}\langle\delta[\mathbf{r} + \mathbf{R}_n(0) - \mathbf{R}_n(t)]\rangle \quad (3)$$

where $\langle\ \rangle$ denotes thermal averaging, N is the total number of particles (for us, a particle is a hydrogen atom), and $\mathbf{R}_n(t)$ is the position of the particle n at time t. In this approximation, $S_{inc}(\mathbf{Q}, \omega)$, as given by Eq. 2, must be corrected by a factor $\exp(-\hbar\omega/2k_BT)$ to account for the usual detailed balance condition. Equations 1–3 indicate how the movements of particles in the sample are related to the measured neutron intensity. In particular, if all scatterers remain immobile, $G_s(\mathbf{r}, t)$ reduces to $\delta(\mathbf{r})$ and $S_{inc}(\mathbf{Q}, \omega)$ to $\delta(\omega)$: the scattering is purely elastic, there is no energy transfer, and $S_{inc}(\mathbf{Q}, \omega)$ is independent of $\mathbf{Q}$. This is a trivial example of a general sum law for incoherent scattering, that is, the integral over ω of $S_{inc}(\mathbf{Q}, \omega)$ remains equal to unity at any value of $\mathbf{Q}$.

Quasielastic scattering

It is usual to simplify the interpretation of data by separating the different kinds of contributions to motion according to their time scales and amplitudes, and subsequently making the hypothesis that these contributions are essentially not coupled between each other. Thus vibrational motions occurring in the 10-fs time scale in a protein may safely be considered as independent from diffusive-type motions due to changes in conformational states of its side chains, which may occur in the picosecond time scale. This differentiation leads to the separation of a spectrum at a given $\mathbf{Q}$ between inelastic scattering (due to vibrational motions, meaning in theory discrete values of scattering energies), quasielastic scattering (arising from diffusive motions leading to a Doppler effect energy modification of the scattered neutron wave), and elastic scattering in the case of confined scatterers (related to the limited volume sampled by each scatterer). In mathematical terms, the independence between the two types of motions, vibrational and diffusive, leads to a total scattering function expressed as the convolution of the respective scattering functions $S_{inc}(\mathbf{Q}, \omega) = S_{vib,inc}(\mathbf{Q}, \omega) \otimes S_{diff,inc}(\mathbf{Q}, \omega)$. In the quasielastic region of the spectrum (i.e., $/\Delta E/ \leq 0.5$–2 meV), the influence of the convolution with the vibrational spectral lines is essentially contained in the Debye-Waller factor, D.W. $= \exp\{-\langle u^2\rangle Q^2/3\}$, which is simply a scaling factor that does not modify the shape of the quasielastic scattering function, in an additive energy-independent background, $B(\mathbf{Q})$, due to the vibrational modes of lowest energy or lattice phonons (Bée, 1988). Hence,

$$S_{q.e.,inc}(\mathbf{Q}, \omega) = e^{-\langle u^2\rangle Q^2/3}[S_{diff.,inc}(\mathbf{Q}, \omega) + B(\mathbf{Q})] \quad (4)$$

where $S_{diff.,inc}(\mathbf{Q}, \omega)$ arises from diffusive motions in the absence of vibrational modes and $\langle u^2\rangle$ stands for the mean square amplitude of vibration.

Data analysis

Solvent subtraction

One of the difficulties in working with protein solutions is the considerable "parasitic" contribution of bulk solvent to the scattering. Despite the fact that the solvent does not contain hydrogen nuclei, its integrated contribution in the quasielastic region ranges from 40% at low Q to 65% at high Q. It is thus of utmost importance to accurately account for this contribution. We have chosen to subtract it from the protein solution spectra by a separate measurement on a pure solvent solution, rather than fitting it with a separate scattering function. To minimize systematic errors, the measurements were performed in the same cell, first for the solvent, then for the protein solution. After respective normalizations for the number of incident neutrons, the final scattering function for the protein was obtained by the following relation:

$$S_{protein}(Q, \omega) = S_{solution}(Q, \omega) - (1 - \nu) \times S_{solvent}(Q, \omega). \quad (5)$$

The factor ν accounts for the fact that the amount of bulk solvent in the protein solution cell is less than in the pure solvent cell. The fraction of bulk water, ν, thus removed by the introduction of proteins was determined by the following procedure. The volumes of "dry" lysozyme and myoglobin in solution were first determined from the tabulated volumes of amino acids found by Jacrot (1976). From these values, the specific volumes of the "dry" proteins were found to be 0.732 cm^3/g and 0.763 cm^3/g for lysozyme and myoglobin, respectively. From the protein concentration, it is then possible to deduce the fraction of solvent volume replaced by protein molecules. The fraction of remaining solvent amounts to 95.4% and

95.3% for lysozyme and myoglobin, respectively. We then make the approximation that, in the picosecond time range, water molecules situated beyond the second protein hydration shell display the same dynamics as pure bulk water. Considering that ~97% of solvent is constituted by such water molecules, the respective fractions of bulk solvent become 92.5% and 92.4%. These last values were used for the constant v in Eq. (5).

Global Brownian motions

The second difficulty in dealing with protein solutions arises from the Brownian motion of the whole proteins. In a hydrated powder, proteins are globally confined, and what is measured from quasielastic neutron scattering is the direct consequence of their internal thermal motions. Conversely, proteins are able to diffuse freely in a solution, and this global motion causes an extra quasielastic broadening in addition to that due to the internal motions. Therefore, to compare the protein internal dynamics to that in hydrated powders, it is necessary to deconvolute in some way the measured $S_{\text{diff,inc}}(Q, \omega)$ by the scattering function arising from global motions. To do so, we have to hypothesize that internal dynamics is essentially independent of the Brownian motion of the whole protein. This seems reasonable, because the diffusion motions for such large molecules as proteins are known to be in the 0.05–1-ns range in the Q range of interest (Cantor and Schimmel, 1980), whereas the time scale of the internal motions is more in the 10-ps range.

The expected shape and variation with Q of the incoherent scattering function due to Brownian translational diffusion of a molecule are a Lorentzian function with a half-width at half-maximum (HWHM), $\Gamma(Q) = D_S Q^2$. Here, D_S is the self-diffusion constant given by the Einstein relation $D_S = k_B \cdot T/6\pi \cdot R \cdot \eta$, where R is the hydrodynamic radius of the diffusing particle and η is the solvent viscosity. In a global translational diffusion, every atom experiences the same motion, which justifies why the macroscopic parameter, D_S, may intervene in a single particle function as $\Gamma(Q)$. Moreover, for a diffusing, dense, spherically shaped molecule, we have numerically checked that its self-rotation motion, characterized by the Debye-Stokes-Einstein relation $D_{\text{rot}} = k_B \cdot T/8\pi \cdot R^3 \cdot \eta$, does not essentially modify the Lorentzian shape of the scattering function, or its Q-variation, but increases its width, leading to an apparent diffusion constant, D_{app}, slightly higher than D_S (Appendix). This is good news for our deconvolution problem, because we can now write the total scattering function for the protein in solution as

$$S_{\text{diff,inc}}(Q, \omega) = \mathcal{L}(Q, \omega) \otimes S_{\text{internal}}(Q, \omega) \tag{6}$$

where $\mathcal{L}(Q, \omega)$ approximates both translational and rotational motions, and check from the fit to the experimental data that $\mathcal{L}(Q, \omega)$ has the expected width variation with Q. If this is the case, then the relevant comparison with hydrated powders should only concern $S_{\text{internal}}(Q, \omega)$. We describe in the following section the fitting model for both the total scattering function from hydrated powders and the "internal" part of the scattering function for solutions.

Internal motions

One of the main characteristics of the internal motions of a well-structured molecule is the confinment of the scatterers within a certain volume of space. This means that, at infinite times, the probability of finding the scatterer within this volume is equal to unity. In terms of scattering function, this is equivalent to the existence of a purely elastic contribution to $S_{\text{internal}}(Q, \omega)$, and the variation of this contribution with Q depends on the shape of the restrictive volume. The really quasielastic part of $S_{\text{internal}}(Q, \omega)$ reveals the time scale and the amplitudes of scatterer fluctuations within this volume. In a phenomenological approach, the quasielastic part may be chosen to be a Lorentzian function, $L_{\text{internal}}(Q, \omega)$, provided the energy range of fitting is not too wide, so that inelastic features are not misincluded in the model. Even in this case, there is still a contribution arising from large-scale modes of vibration (lattice modes in solid-state physics), which introduces a small flat background, $B(Q)$, in the quasielastic region, with a Q^2 variation in intensity (see Eq. 4). The model for $S_{\text{internal}}(Q, \omega)$ is, finally,

$$S_{\text{internal}}(Q, \omega) = A_0(Q) \cdot \delta(\omega) + (1 - A_0(Q)) \cdot L_{\text{internal}}(Q, \omega). \tag{7}$$

From using Eqs. 4 and 6, the quasielastic experimental data are fitted for hydrated powders by

$$S_{\text{inc,exp}}(Q, \omega) = P(Q) \cdot e^{-\hbar\omega/2k_BT} \cdot [S_{\text{internal}}(Q, \omega) + B(Q)] \otimes S_{\text{res}}(Q, \omega), \tag{8}$$

and for protein solutions by

$$S_{\text{inc,exp}}(Q, \omega) = P(Q) \cdot e^{-\hbar\omega/2k_BT} \cdot [\mathcal{L}(Q, \omega) \otimes S_{\text{internal}}(Q, \omega) + B(Q)] \otimes S_{\text{res}}(Q, \omega), \tag{8bis}$$

where $P(Q) = e^{-\langle u^2 \rangle Q^2/3}$ if coherent scattering is neglected, and $S_{\text{res}}(Q, \omega)$ is the resolution function obtained from vanadium scattering. The fitting procedure is performed for each value of Q independently (to be precise, the spectra are at constant angle, but in the quasielastic region, this almost corresponds to constant Q). Hence no a priori model for Q dependence is introduced into the fit, neither for $A_0(Q)$, nor for the Lorentzian functions. Whether the variations with Q resulting from the fit do or do not follow a theoretical model should therefore be considered as a relevant result, not as an initial constraint. The use of a single Lorentzian function $L_{\text{internal}}(Q, \omega)$ is justified by our concern to derive simple order parameters that might be comparable from one protein to another and from one hydration level to another. We are aware that this Lorentzian reflects only an average of different kinds of diffusing motions, the details of which are inaccessible to our technique.

Transfer energy range

The fitting region itself may influence the width and proportion of the quasielastic scattering. This is expected in a sense, because widening the energy region of fit forces the model to include additional diffusive motions with lower correlation times under the Lorentzian envelope. Actually, the frontier between what is inelastic and what becomes quasielastic is rather blurred. However, it seems acceptable that the narrower the fitting region is, the fewer inelastic features should be artificially included in the fit. This has led us to perform the fit for $|\hbar\omega| \leq 1.0$ meV, which corresponds roughly to 20 times the HWHM resolution. We have noticed that, for a wider range, the single Lorentzian model slightly fails to fit the highest energy data, with the model constantly remaining at a value too low compared to the measured data. We have interpreted this as the occurrence of inelastic features at these values of transfer energy. Fig. 1 presents examples of fitted spectra.

Independent measurement of $\langle u^2 \rangle$

If only incoherent scattering were present, the value of $\langle u^2 \rangle$ could be directly derived from the variation of $P(Q)$ in the expressions 8 and 8bis. However, although incoherent scattering is the predominant phenomenon in the present experiment, it is not possible to completely avoid coherent scattering. Unlike incoherent scattering, the integral of coherent scattering over ω, $S_{\text{coh}}(Q)$, depends on Q and is related to the atomic structure of the sample by the square of a Fourier transform. If we make the assumption that coherent scattering has little effect on the proportion between the different components (elastic and quasielastic) in the quasielastic region, then its main consequence is to modulate the variation of $P(Q)$ with Q in expressions 8 and 8bis. It is therefore not possible to obtain a reliable value for $\langle u^2 \rangle$ from $P(Q)$. However, the Debye-Waller factor is common to both coherent and incoherent scattering. The total quasielastic scattered intensity

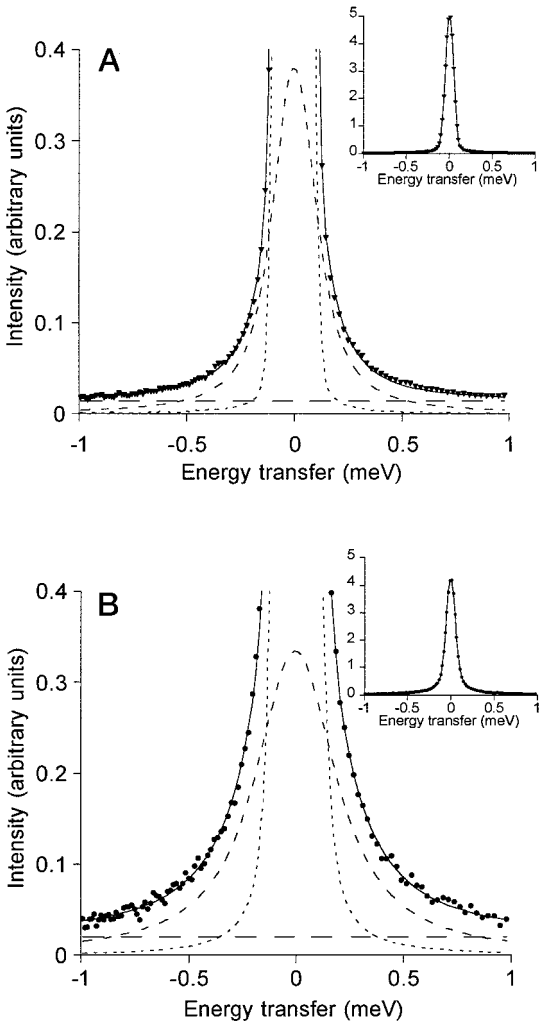

FIGURE 1 Quasielastic scattering intensity recorded at a constant angle ($Q_0 = 1.35$ Å^{-1}) with IN6 for (*A*) myoglobin 0.43 g/g powder sample and (*B*) myoglobin solution sample after solvent scattering subtraction. The phenomenological fit represented by the solid line is based on (*A*) Eq. 8 and (*B*) Eq. 8bis. The different components correspond to (*A*) the elastic peak (*dotted line*), the internal Lorentzian function (*dashed line*), and the flat background (*large dashed line*); and (*B*) the global motion Lorentzian $\mathcal{L}(Q, \omega)$ (*dotted line*), the internal Lorentzian function $L_{\text{internal}}(Q, \omega)$ convoluted by $\mathcal{L}(Q, \omega)$ (*dashed line*), and the flat background (*large dashed line*).

can be written as

$$S_{\text{q.e.,tot}}(Q) = e^{-\langle u^2\rangle Q^2/3} \cdot S_{\text{tot}}(Q), \tag{9}$$

where $S_{\text{tot}}(Q)$ is the integral of total (incoherent + coherent) scattering over ω. Therefore, the Debye-Waller factor is simply given by the ratio of $S_{\text{q.e.,tot}}(Q)$ over $S_{\text{tot}}(Q)$, were both quantities are obtained directly from numerical integration of the experimental data. In practice, $S_{\text{q.e.,tot}}(Q)$ is obtained by an integration over $|\hbar\omega| \leq 1$ meV and $S_{\text{tot}}(Q)$ over $|\hbar\omega| \leq 20$ meV, after conversion of the data from the (θ, ω) basis to the (Q, ω) basis with the program Ingrid from ILL (Grenoble).

Small-angle x-ray scattering

Small-angle x-ray scattering (SAXS) experiments have been performed to test the quality of the solution specimens used in the neutron experiments. The synchrotron radiation SAXS data were collected following standard procedures on the D24 spectrometer at LURE (University of Paris-Sud, Orsay, France), using a wavelength of 1.488 Å. The scattering patterns covered the range of momentum transfer 0.01 Å$^{-1} < Q < 0.3$ Å^{-1}. The data were corrected for the detector response, and the buffer scattering was subtracted. The SAXS curves show clearly the absence of aggregation in the samples after the neutron experiments.

Quasielastic light scattering

Quasielastic light scattering (QELS) measurements were performed on the myoglobin solution sample, to measure the translational diffusion constant, D_0. The data were collected at LLB (CEA Saclay, Gif-sur-Yvette, France) with a homemade light scattering device, using a polarized light source (Kr^+, wavelength $\lambda_0 = 647$ nm) at a scattering angle of 150°. QELS experiments were performed using the self-beat technique, with the time-averaged autocorrelation function of the scattered intensity obtained with a Malvern 7032 multicorrelator.

RESULTS

Global motions of protein in solution

The linewidth of the narrow Lorentzian function $\mathcal{L}(Q, \omega)$ accounting for protein global motions has been derived as a function of Q (Fig. 2), using the fitting procedure on the protein solution IQENS data. The evolution with Q is well accounted for by the diffusion model presented in the Data Analysis section, $\Gamma = D_{\text{app}}Q^2$. The apparent diffusion constants found are $D_{\text{app}} = 5.4 \pm 0.1\ 10^{-3}$ meV · Å^2, i.e., $8.2 \pm 0.2\ 10^{-7}$ cm^2/s for myoglobin, and $D_{\text{app}} = 6.0 \pm 0.1\ 10^{-3}$ meV · Å^2, i.e., $9.1 \pm 0.2\ 10^{-7}$ cm^2/s for lysozyme. These diffusion constants are on the same order of magnitude as those given by other techniques in the literature for the same proteins in solution, which gave us confidence in our fitting model. From laminar flow experiments on myoglobin in

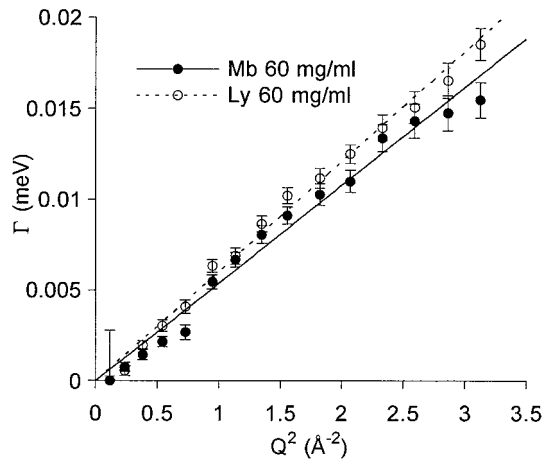

FIGURE 2 Half-width at half-maximum, Γ, of the Lorentzian $\mathcal{L}(Q, \omega)$, which accounts for global motion of protein in solution, and results from the phenomenological fit based on Eq. 8bis. For both lysozyme and myoglobin solution samples, it appears that $\Gamma(Q)$ is a quadratic function of Q, as expected for a free diffusion motion. The fitted slope of Γ versus Q^2 is indicated by the solid or dotted line for the myoglobin or lysozyme solution sample, respectively, and gives the value of the apparent diffusion constant, D_{app}, $8.2 \pm 0.2 \times 10^{-7}$ cm^2/s and $9.1 \pm 0.2 \times 10^{-7}$ cm^2/s, respectively.

water at 25°C, Walters et al. (1984) give $10.3 \pm 0.2\ 10^{-7}$ cm^2/s for D_0, the translational diffusion constant at infinite dilution. From dynamic light scattering (DLS) measurements, Kuehner et al. (1997) find a value for D_0 of $13.0 \pm 0.5\ 10^{-7}$ cm^2/s for lysozyme in water at 25°C.

To compare the literature values with our IQENS values, it is first necessary to correct for the difference in viscosity between water and heavy water and for the different temperatures. Thus, as $\eta_{20°C}(D_2O) = 1.247$ cp (Millero et al., 1971) and $\eta_{25°C}(H_2O) = 0.8904$ cp (Weast, 1974) (1 cp (Centipoise) $= 10^{-2}$ g/(s · cm)), which gives $\eta_{20°C}(D_2O)/\eta_{25°C}(H_2O) = 1.4$, the expected values of D_0 in heavy water at 20°C are $7.4 \pm 0.2\ 10^{-7}$ cm^2/s for myoglobin and $9.3 \pm 0.4\ 10^{-7}$ cm^2/s for lysozyme. We measured by DLS at 20°C the diffusion coefficients of the myoglobin solutions used for the neutron experiments, after a 10-fold dilution in pure D_2O. We obtained $D_0 = 7.2 \pm 0.3\ 10^{-7}$ cm^2/s, which is just slightly lower than the previous value extrapolated from laminar flow experiments. We shall therefore keep for both proteins the values given by DLS.

Second, we have to account for the effect of concentration and the effect of rotational motions, which we describe now. Let us first recall that neutron incoherent scattering is, in essence, not sensitive to correlations between distinct scatterers, whereas photon correlation spectroscopy is a coherent scattering technique and is therefore sensitive to dynamics and to interparticle static interactions as well. The respective translational dynamic constants accounted for by these two techniques, the self-diffusion constant, D_S, and the collective diffusion constant, D_C, are therefore essentially different in nature. However, they both tend to D_0 at infinite dilution, which is expected because in these conditions there are no interparticle interactions. D_0 is easily extrapolated from the values of D_C obtained by photon correlation spectroscopy. The values of D_0 given above are extrapolated values. From D_0, we may predict the value of D_S in the present IQENS experiment by accounting for the effect of finite concentration of the solutions. Venkatesan et al. have published a theoretical development on the variation of D_S upon concentration and attractive or repulsive colloidal interactions. One result is that, in the case of repulsive interactions, the ratio $D_S(\phi)/D_0$, where D_0 is the diffusion constant at infinite dilution, is $(1 - \lambda.\phi)$, where ϕ is the particle volumic fraction and λ is a positive scalar lower than 1.73. Venkatesan et al. show that the stronger the repulsive interactions, the lower is λ; the value of 1.73 represents the limiting case of noninteracting hard spheres. For the present myoglobin and lysozyme solutions, $\phi = 4.7\%$ and $\phi = 4.6\%$, respectively. SAXS measurements performed on the neutron samples after the IQENS experiment showed a large peak, characteristic of repulsive interparticle interactions for the lysozyme solution, whereas the myoglobin solution presents essentially no interparticle interactions. This is perfectly coherent with the state of charge of each protein described in the Sample Preparation section. The predicted values for D_S are then $0.92D_0$ for myoglobin and between D_0 and $0.92D_0$ for lysozyme, probably closer to D_0 than $0.92D_0$, even if the strength of the repulsive interactions has not been quantified. Then, taking into account the neutron sample concentrations, the expected values of D_S are 6.6×10^{-7} cm^2/s for myoglobin and comprised between 8.5×10^{-7} and 9.3×10^{-7} cm^2/s for lysozyme.

As stated in the Data Analysis section, IQENS diffusion constants include translational as well as rotational effects, whereas D_S only characterizes the translational motions of the particles. We show in the Appendix that the effect of rotations on hard dense spheres is to increase the value of D_{app} measured by IQENS by ~27% with respect to D_S. Then, if we finally account for this effect, we obtain expected values for D_{app} of $1.27 \times 6.6 = 8.4 \times 10^{-7}$ cm^2/s for myoglobin and between 10.8×10^{-7} cm^2/s and 11.8×10^{-7} cm^2/s for lysozyme. The agreement with the experimental IQENS is now excellent for myoglobin, and a little less so for lysozyme, which may be due to a nontrivial effect of the repulsive interparticle interactions on global rotations. However, at this point, we believe that the effect of global motions in the present protein solutions has been properly deconvoluted, so we can now compare the internal picosecond dynamics of powders and solutions.

Internal motions

As we stated in the Data Analysis section, the internal motions measured by our experiment belong to the picosecond time scale. These motions are characterized at a given Q, both in powder and in solution, by the width $\Gamma_{internal}(Q)$ of the Lorentzian function $L_{internal}(Q, \omega)$, which may be linked to the magnitude of an average correlation time, and by the contribution of $L_{internal}(Q, \omega)$ to the total scattering, $(1 - A_0(Q))$, which depends on the amount of diffusing scatterers. The variation over Q of these two parameters may also give indications of the nature of the motions. For example, a Q-independent linewidth may be the signature of jump motions between two or three definite sites. More precisely, if we consider the case of methyl hydrogens making 120° jumps about the threefold axis, Γ is independent of Q and is equal to three times the inverse of the residence time on each site. On the other hand, a continuous diffusive motion of a scatterer within a restrained volume of space generally causes an increase of the linewidth with Q and tends to a finite extrapolated value of the linewidth at $Q = 0$. In particular, the model of free diffusion within a sphere has been successfully used to model alkyl chains motions in columnar mesophases (Carpentier et al., 1989), which gives it some relevance in modeling protein sidechain motions. The restrained diffusion contrasts with the case of free diffusion in an infinite volume, where the linewidth vanishes at $Q = 0$ (see previous section).

The variation with Q of the Lorentzian integrated intensity (equal to $1 - A_0$ in our approach) is related to the amplitude and shape of the scatterer trajectory. For instance, a free diffusion motion within a sphere of finite size implies

$A_0(Q) = [3j_1(Qa)/Qa]^2$, where j_1 is the first-order Bessel spherical function of the first kind, and a is the sphere radius (Volino and Dianoux, 1980). This function equals unity at $Q = 0$ and has a null value at $Q \approx 4/a$. A three-sites jump model would tend to $A_0(Q) = \frac{1}{3}[1 + 2j_0(Qa\sqrt{3})]$, where $j_0(x) = \sin(x)/x$, and a is the radius of the circle containing the three sites. In this case, there is a finite marked minimum at $Q \approx 2.6/a$. A different type of motion would give a different variation of A_0 with Q. Thus, in principle, by analyzing $A_0(Q)$, we should be able to distinguish between several types of motion. This is true in simple cases, but only if the accessible Q range is large. As a matter of fact, the distinct models of $A_0(Q)$ substantially differ from a Gaussian only at values of Qa higher than ~2, where a is a typical size of the volume explored by the scatterer. The analysis is even more complicated in a system as complex as a protein because of the heterogeneity of existing motions. Because we only observe an average of all types of motions, the variation of A_0 with Q may only give very rough information on the shape of motion. Therefore, whatever model we employ, it is only phenomenological and more useful for comparison between different hydration states than for an atomic interpretation of the different kinds of hydrogen motions.

In what follows, we describe the evolution of $\Gamma_{\text{internal}}(Q)$, $A_0(Q)$, $B(Q)$, and $\langle u^2 \rangle$ with Q derived from the fits of $S_{\text{exp}}(Q, \omega)$ by the expressions 8, 8bis, and 9, and we analyze these quantities by using the two preceding models (three-site jumps and free diffusion in a sphere).

Quasielastic width

The Lorentzian linewidth (HWHM), $\Gamma_{\text{internal}}(Q)$, increases slightly with Q in hydrated powders of both proteins, with no detectable influence of the hydration level, whereas it seems to remain constant for the dry myoglobin sample. Its extrapolated value at $Q = 0$ is almost the same for all powders and is on the order of 70 μeV, which corresponds to the inverse of a correlation time $\tau = 9.4$ ps or to a residence time $\tau_{\text{res}} = 28.2$ ps in the framework of the three-sites jump model. The increase with Q is more pronounced for lysozyme than for myoglobin, giving a value of HWHM at $Q = 2$ Å^{-1} of 125 μeV for the former and 115 μeV for the latter (Fig. 3). An increase with Q comparable to the most hydrated powders seems to hold for solutions. However, the extrapolated value at $Q = 0$, ~150 μeV for both myoglobin and lysozyme, is twice that obtained for hydrated powders, with a corresponding correlation time of 4.4 ps. The absence of distinguishable variation in Γ_{internal} with Q for the dry sample suggests that motions, in this case, are mainly of the reorientational type, presumably three-site jump motions of methyl groups. Conversely, the increase in Γ_{internal} with Q indicates the existence of diffusive motions in all hydrated powders as well as in solution. The lower correlation time observed at low Q for proteins in solution reflects the occurrence of faster motions than in hydrated powders.

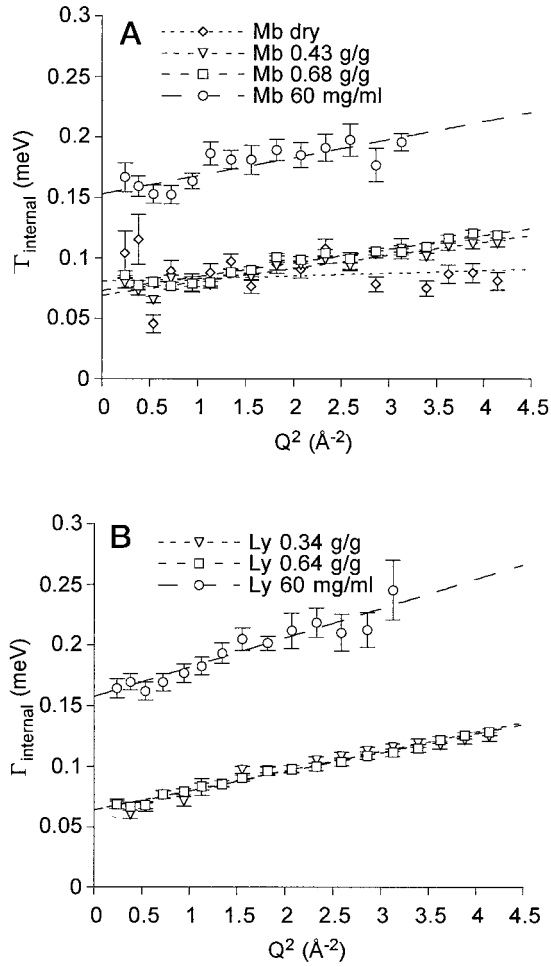

FIGURE 3 Half-width at half-maximum, Γ_{internal}, of the internal motion Lorentzian $L_{\text{internal}}(Q, \omega)$, resulting from the phenomenological fit based on Eq. 8 and Eq. 8bis, for (*A*) myoglobin samples and (*B*) lysozyme samples. The lines are deduced from a linear fitting to the "experimental" values and are only a guide for the eyes. Except for the dry myoglobin sample, Γ_{internal} increases with Q^2, which characterizes the presence of local diffusive motions as soon as the protein is hydrated. In the case of dry myoglobin, Γ_{internal} is almost constant, as expected from a reorientational type of motion. The inverse of Γ_{internal} gives the correlation time of the motions. In solutions, the correlation time extrapolated at $Q = 0$ is ~4.4 ps, more than twice that in powders.

Quasielastic amplitude

Fig. 4 shows the "experimental" A_0 as a function of Q for all samples. These values have been fitted by both the free diffusion in a sphere and the three-site jump models, but considering a distribution of the characteristic length a instead of a unique value. This is a way to account for the heterogeneity of the hydrogen motions in the protein and to better reproduce the experimental $A_0(Q)$. The distribution of a was taken as a Gaussian function, $g(a) = \sigma^{-1}(2\pi)^{-0.5}\exp(-(a - c)^2/2\sigma^2)$ with its center, c (imposed as positive), and variance, σ, as fitting parameters. In addition to these functions accounting for the moving scatterers, we introduce a third fitting parameter, p, not described in the Data Analysis section for simplicity, which is constant with

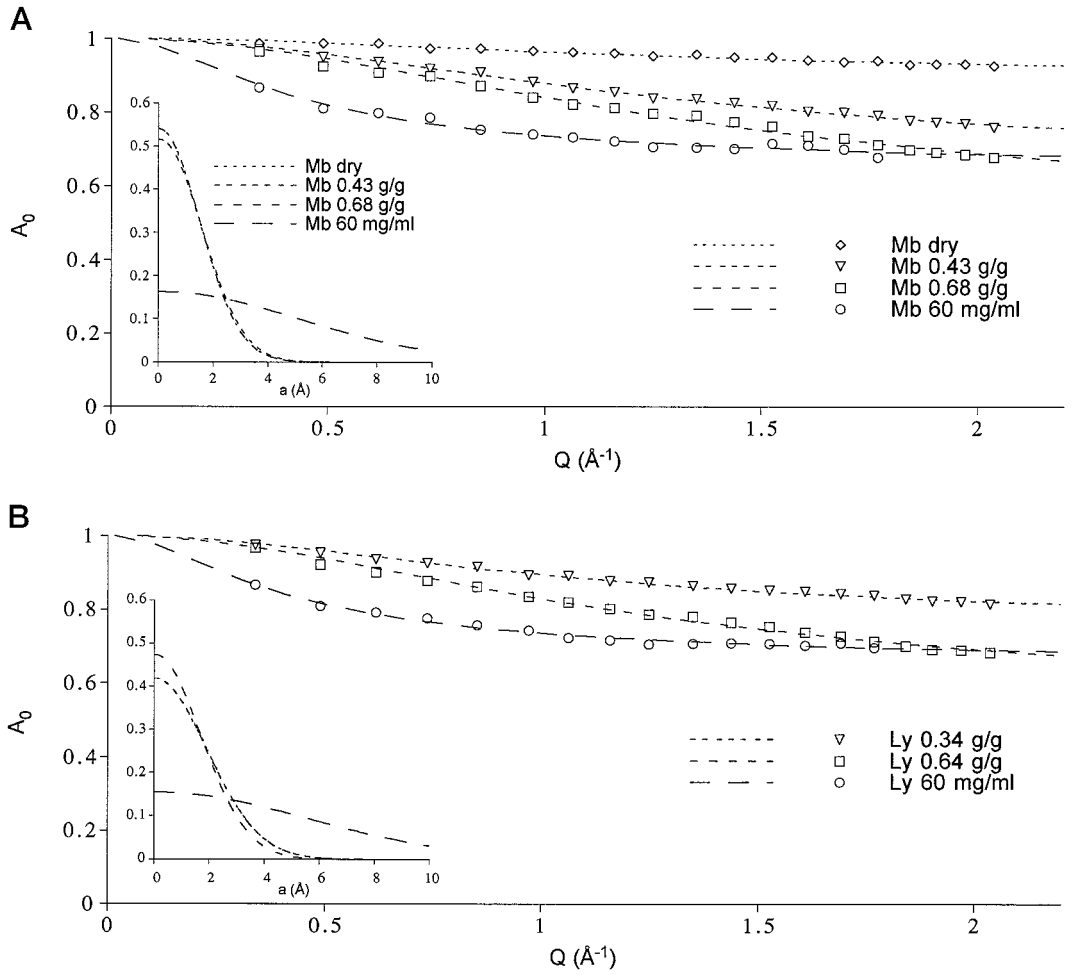

FIGURE 4 Values of A_0 as a function of Q, resulting from the phenomenological fit based on Eq. 8 and Eq. 8bis, for (*A*) myoglobin samples and (*B*) lysozyme samples. The fitting lines result from the model of free diffusion in a sphere of radius a, with respective radii distributions given by the functions shown in the inset. A_0 decreases in solution at a lower Q than in powders, suggesting that the average amplitude of the internal motions is higher in solution. This is translated in the model by a distribution in solution about three times larger than in powders.

Q. This parameter represents the fraction of nonexchanged hydrogens in the protein that are only submitted to motions faster than a few picoseconds (vibrational motions, for example) or to internal diffusive motions much slower than the experimental resolution is able to detect. Scattering by these "immobile" hydrogens produces a constant contribution to A_0.

The two models fit each experimental set of data with the same fit quality, but for clarity, the fitting curves are shown for each sample in Fig. 4 only for the model of free diffusion in a sphere. The fit is particularly good for the powders with a hydration below 0.45 g/g and for the solutions. The fit for powders at 0.6–0.7 g/g is only fair. In all cases, the fit with a single value for the radius, a, instead of a distribution, is not convincing (not shown). During the fitting procedure, the center, c, of the Gaussian radius distribution invariably tends to zero for all fitted samples and for both models. This means that a nonnegligible part of the diffusive motions that we detect here are of very low amplitude. However, in all cases, the distributions are large enough to account for typical distances expected for methyl hydrogen flips, for which $a = 0.99$ Å, or for diffusive liquid-like motions of surface side chains.

Global comparison between the two models. Table 1 gives the fitted values of σ and p. The average value of the radius, a, is then given by $\sigma \cdot (2/\pi)^{0.5}$, and its r.m.s. value by σ. Although the two models produce almost exactly the same fitting curves, the parameters used in each case differ in amplitude. For a given protein and a given hydration level, the values of σ and p are systematically lower in the three-site jump model than in the model of free diffusion in a sphere. That the values of σ differ is not too surprising, because a does not represent the same type of radius in each of the two models. More surprising is that the value of p, which is supposed to reflect a physical quantity, in fact depends on the model used. None of these models, of course, is able by itself to represent the reality. At most, we may think of the actual dynamics as a combination of them, the free diffusion model being more adequate at high values of a, and the site-jump at low values of a. But the weighting

TABLE 1 Values of the parameters σ and p deduced from fitting the variation of A_0 with Q by two different models, free diffusion in a sphere and three-site jump

	Lysozyme			Myoglobin			
Hydr. level	0.34 g/g	0.64 g/g	∞	Dry	0.43 g/g	0.68 g/g	∞
Dif. σ (Å)	1.91 ± 0.02	1.68 ± 0.01	5.54 ± 0.03	1.48 ± 0.01	1.53 ± 0.01	1.47 ± 0.03	5.19 ± 0.03
p	0.73 ± 0.01	0.51 ± 0.01	0.65 ± 0.01	0.88 ± 0.01	0.61 ± 0.01	0.46 ± 0.03	0.64 ± 0.01
Jum. σ (Å)	1.26 ± 0.01	1.08 ± 0.01	3.12 ± 0.03	0.96 ± 0.01	1.00 ± 0.01	0.96 ± 0.03	2.95 ± 0.03
p	0.66 ± 0.01	0.36 ± 0.01	0.50 ± 0.01	0.85 ± 0.01	0.51 ± 0.01	0.32 ± 0.03	0.49 ± 0.01

factors governing this combination cannot be determined by IQENS. In fact, the information given by IQENS lies in the evolution of the parameters σ and p with the hydration level, which, indeed, is common to both models.

Evolution of σ and p with the hydration level. We shall examine here the case of myoglobin, for which we have four samples, and more particularly compare the dry, 0.43 g/g, and solution samples. The case of 0.68 g/g hydration will be commented on afterward.

From Table 1 it appears that the width, σ, of the motion amplitudes distribution is hardly lower for dry than for 0.43 g/g myoglobin in both models, whereas it is much higher for the solution. At the same time, the fraction, p, of "immobile" scatterers decreases when the powder hydration is raised to 0.43 g/g, then remains essentially the same in solution. Thus at 0.43 g/g hydration, all protein hydrogens "able to move" within the time scale of the observation do move, whereas only part of them, about one-third, can do so in the dry powder. On the other hand, there is not much difference in the amplitudes of motion possible in the two cases, dry and 0.43 g/g. The effect of the water molecules is therefore to allow a higher number of motions to occur at the same time, and not to modify significantly the amplitude of preexisting motions. On the contrary, p does not change when going from the hydrated powder to solution, but instead, quite large motional amplitudes are permitted on the same time scale. In this case, the role of the additional water molecules is probably to facilitate the diffusion of hydrogen atoms or their jumps from one conformation to another. Hence, within the same time window, a hydrogen atom of the protein in solution is able to cover a larger distance than the same atom at 0.43 g/g hydration. But the number of atoms subject to diffusive motions does not change between 0.43 g/g and solution.

The lower values of p obtained at 0.68 g/g hydration make us suspect that global motions take place already at this level of hydration, because there cannot be more diffusing hydrogen atoms in a solvated powder than in solution. In this case, the powder model (without a Lorentzian model for global motions) becomes inadequate, as will be discussed later.

The case of lysozyme. After the analysis of the myoglobin data, we realized that the data collected on lysozyme were difficult to interpret by themselves, mainly because we did not have a dry sample to compare to the 0.34 g/g hydration sample. However, in light of the preceding chapter, we can understand the lysozyme results in the same way as those for myoglobin. Thus the value of p in lysozyme at 0.34 g/g hydration is higher than in solution, but remains between p of myoglobin in dry and 0.43 g/g powders. This means that, at 0.34 g/g hydration in lysozyme, the hydrogen atoms "able to move" still lack some water molecules needed to be able to move all at the same time. The values of σ are higher for lysozyme than for myoglobin samples, suggesting that lysozyme would be, on average, more flexible. This is also supported by the higher increase in $\Gamma_{\text{internal}}(Q)$ with Q for lysozyme than for myoglobin.

Background

As discussed in Materials and Methods, the evolution of the background should be quadratic with Q. This is indeed the case for powders as well as for solutions (Fig. 5). In hydrated powders, the slope versus Q^2 of the background increases upon hydration, independently of the protein. This indicates an increase in amplitude of the lattice modes, probably due to a softening effect of water on these modes of low frequency. In solutions, the extrapolation of the background at $Q = 0$ is not zero, probably because of the existence of a small amount of multiple scattering, which produces some Q-independent inelastic scattering. The interpretation of the slope versus Q^2 is therefore more hazardous in this case.

Mean square vibrational amplitudes

The Debye-Waller factor has been deduced for each sample from the direct numerical integration of the experimental data, without using any model (see Data Analysis section). Fig. 6 shows, for each sample, the variation of the natural logarithm of the Debye-Waller factor as a function of Q^2. The evolution is clearly linear for the hydrated powders, as expected from theory. The slope gives the value of $\langle u^2 \rangle/3$ for each sample. Let us recall that $\langle u^2 \rangle/3$ accounts here only for the amplitude of the vibrational modes with an energy higher than 1 meV. The value obtained, ~0.055 Å^2, does not depend on the hydration state, or on the type of protein, showing that the softening effect of water is less strong on these "high"-frequency modes. The case of the solution samples is again complicated by the small amount of multiple scattering, which gives an extrapolation at $Q = 0$ of the Debye-Waller factor apparently lower than unity. Again, the

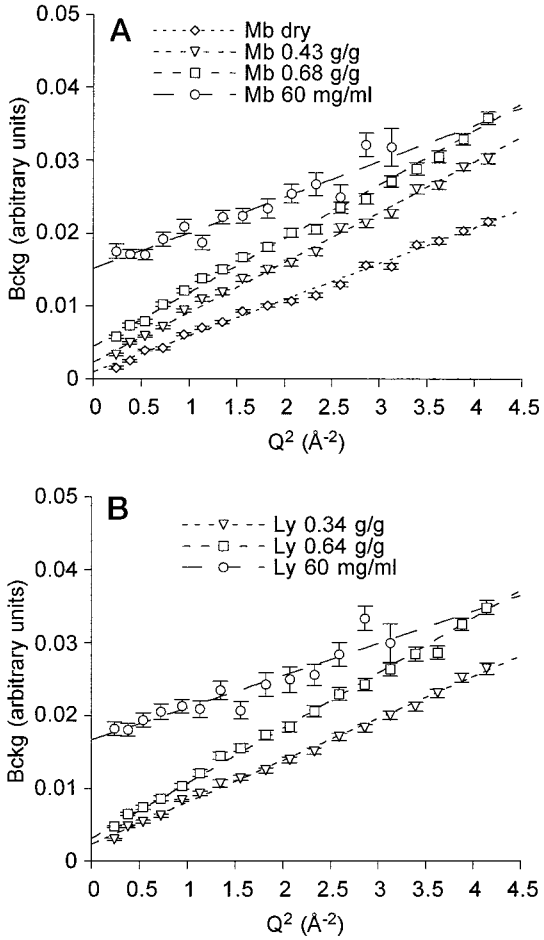

FIGURE 5 Background $B(Q)$, resulting from the phenomenological fit based on Eq. 8 and Eq. 8bis, for (A) myoglobin samples and (B) lysozyme samples. The vertical scale is the same as in Fig. 1. The evolution with Q is remarkably quadratic, as expected from "lattice" modes. The slopes of B versus Q^2 increase with hydration in powders, underlining the strong influence of water on these modes. The values are the following: 4.9×10^{-3} Å^2 (Mb dry), 5.7×10^{-3} Å^2 (Ly 0.34 g/g), 6.9×10^{-3} Å^2 (Mb 0.43 g/g), and 7.5×10^{-3} Å^2 (Ly 0.64 g/g and Mb 0.68 g/g). $B(Q)$ should vanish at $Q = 0$, which is practically the case in the hydrated powders, but not in the solutions. This is presumably due to the existence of a small amount of multiple scattering in the latter case.

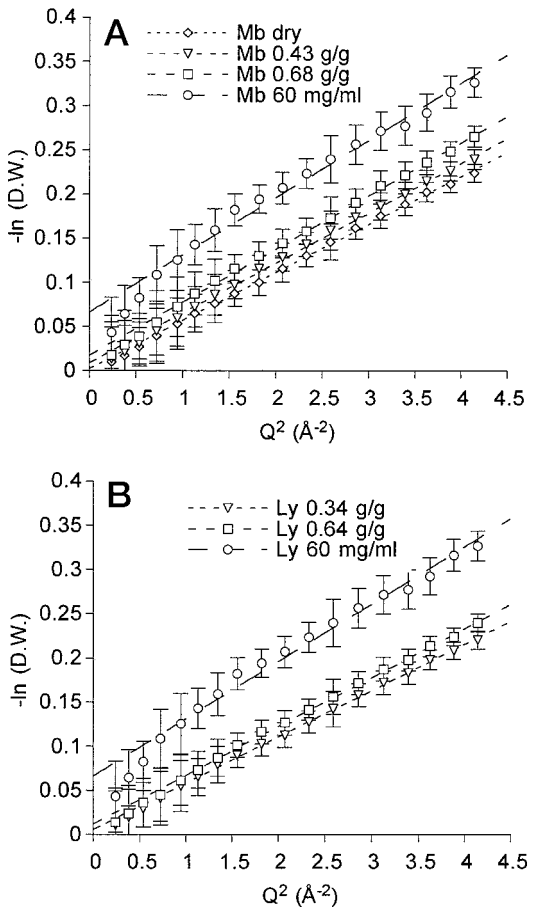

FIGURE 6 Debye-Waller (D.W.) factor calculated from direct integration of the raw experimental data as the ratio of quasielastic scattering ($\Delta E < 1$ meV) over total scattering ($\Delta E < 20$ meV), for (A) myoglobin samples and (B) lysozyme samples. The slope of $-\ln$ (D.W.) versus Q^2 is shown in the figure and gives $\langle u^2 \rangle/3$, where $\langle u^2 \rangle$ is the mean square amplitude of the vibrational motions. The value of $\langle u^2 \rangle$, ~0.17 Å^2, appears to be almost independent on hydration, showing the small influence of water on these high-frequency modes. In solutions, the extrapolation at $Q = 0$ is finite, presumably because of the existence of a small amount of multiple scattering.

apparent value of $\langle u^2 \rangle/3$ should not be completely trusted in this case.

DISCUSSION

It is often believed that, for a given incident neutron energy resolution, any motion with a correlation time higher than the inverse of this resolution should be considered as producing elastic scattering, i.e., it would not be detected and should therefore be ignored. The data treatment that we have presented on solution samples seems to prove the opposite. Here, the correlation times associated with the Brownian motions of the whole proteins are situated between 2 ns and 150 ps, depending on the value of Q, and the spectrometer resolution presents a half-width at half-maximum of 80–140 μeV, corresponding to much lower correlation times, ranging between 50 and 30 ps. Still, the correct diffusion constants could be extracted from the data, which cannot be considered a coincidence. Our interpretation of this apparent contradiction lies in the fact that there is strictly no elastic scattering in the special case of a solution. Schematically, the whole "elastic" peak is broadened by the effect of unconfined global motions. Bearing this in mind, it is not extraordinary that it is possible to detect a much narrower broadening than the resolution. Conversely, a very slow internal motion of confined scatterers should not be detectable, because it would only cause the broadening of a small part of the total "elastic" scattering.

Nevertheless, if we are mostly interested in protein dynamics, the true question is: How much does the treatment including global motions modify the results concerning the internal motions? Clearly, the strength of this influence

should depend on the protein size. Because the diffusion constant is inversely proportional to the particle hydrodynamic radius, the larger the protein is, the lower the broadening of the "elastic" peak will be and the less this treatment will be necessary. However, for small globular proteins such as lysozyme and myoglobin, the global motions must be taken into account. To prove this point, we performed a "powder" data treatment for the solution data, meaning that we considered the sum of an elastic peak and a quasielastic Lorentzian for each value of Q. Above all, the resulting fit is of very poor quality, giving, at every value of Q, a χ^2 value more than twice as large as that obtained with the treatment including the global motions. Fig. 7 compares Γ_{int} and A_0 as a function of Q for both treatments of the myoglobin solution sample. Γ_{int} and A_0 have completely different values. Thus A_0 decreases much more with Q with the "powder" treatment. If we try to fit this variation with the distribution of free diffusion spheres, as in the "global motions" treatment, we find $\sigma = 2.04 \pm 0.01$ Å and $p = 0.11 \pm 0.01$. The distribution width of sphere radii and the number of hydrogen atoms with nondetectable motions appear to be much lower. The width of the quasielastic Lorentzian accounting for the internal motions is much lower, too. Clearly, the conclusions derived from the two treatments would be very different, underlining the necessity to account for the protein Brownian motion. Concerning the powders hydrated at 0.64 and 0.68 g/g, the low value obtained for p may very well arise from the same type of mismodeling as the one exposed above. There might exist, at this level of hydration, some coupling between the internal dynamics and motions of the protein as a whole. This would explain why more hydrogen atoms seem to contribute to the quasielastic scattering attributed to the internal motions in powders than in solution. Once in solution, the internal and external dynamics are decoupled, and the number of contributors to internal dynamics can be separated. The picture emerging from our results and these considerations is described below.

1. Dry myoglobin shows reorientational motion of the nonexchangeable hydrogens, characterized by a quasielastic linewidth constant with Q. The fact that not only vibrational motions are present in a dry protein sample has been also observed by Fitter et al. (1997) on delipidated dry bacteriorhodopsin. They find a correlation time of 5.5 ps, compared to the present 9.4 ps. However, because they do not indicate the variation of the linewidth with Q (indicative of the type of motions), but only the value at $Q = 1.7$ Å^{-1}, the two correlation times may not be directly comparable on a quantitative basis. In our case, the observed motions are most probably due to methyl flips, with a corresponding residence time between flips of 28.2 ps.

2. At 0.4 g/g (i.e., at full hydration of the protein surface by water), compared to the dry protein, the number of moving atoms increases and the type of diffusive motion evolves, according to the different behavior of the linewidth of $L_{internal}$ with Q. Without being too precise, we can state that some confined diffusion appears in addition to the reorientational motion. This diffusion can probably be attributed to surface side chains, which are able now to change their configuration by exchanging their position with that of water molecules. However, the relaxational time related to this phenomenon cannot be decoupled here from the reorientational time arising from the methyl flips, particularly because this itself may change with hydration when hydrophobic side chains are exposed to solvent. The most interesting point at 0.4 g/g is that the number of hydrogen atoms subject to internal diffusive motions (on the

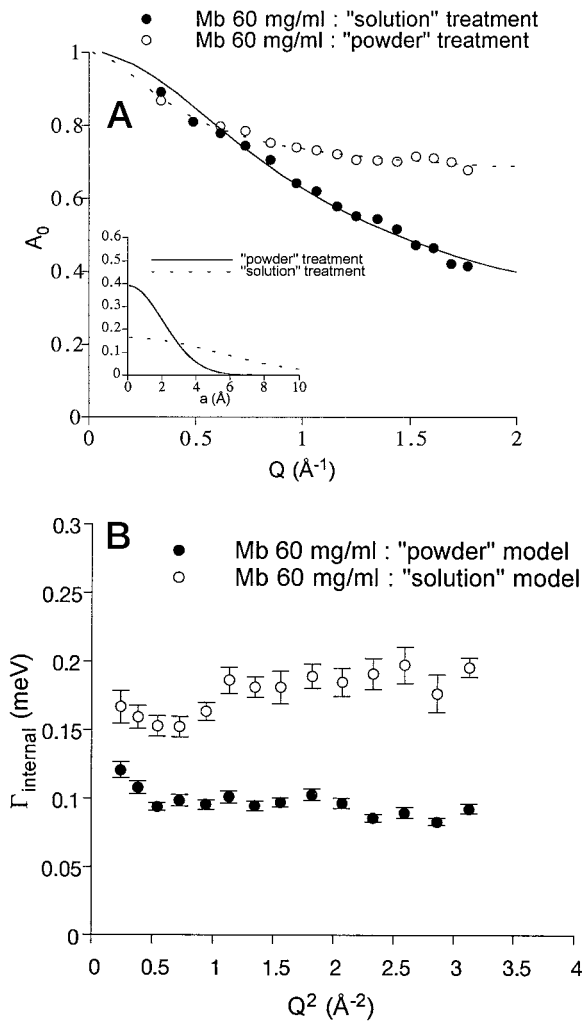

FIGURE 7 Two treatments have been used for the same experimental data from the myoglobin solution sample. The "solution" treatment, based on Eq. 8bis, explicitly accounts for global motions, whereas the "powder" treatment, based on Eq. 8, does not. Not only does the first model fit the experimental scattering function much better for each value of Q (not shown), but accounting for the global motions clearly affects the interpretation of the results. (*A*) Values of A_0 as a function of Q. The fitting lines result from the model of free diffusion in a sphere of radius a, with respective radii distributions given by the functions shown in the inset. The "powder" treatment gives a much narrower distribution and a much lower fraction of nondiffusing hydrogens than the "solution" treatment. (*B*) Half-width at half-maximum, $\Gamma_{internal}$, of the internal motion Lorentzian $L_{internal}(Q, \omega)$. The correlation time appears to be almost twice as high in the "powder" treatment than in the "solution" treatment.

picosecond time scale) is the same as in solution, whereas the amplitude of these diffusive motions is significantly lower and their time scale significantly higher than in solution. This does not contradict the fact that the intrinsic heat capacity of the system (protein + first water layer) does not change upon further hydration (Rupley and Careri, 1991). Thus Rupley and Careri do not discard the possibility that "some motional properties change significantly above hydration level for completion of principal changes in thermodynamic properties" (1991, p. 125). They base their assertion on electron spin resonance measurements of lysozyme with a noncovalently bound spin probe, TEMPONE (Rupley et al., 1980), which show a continuous decrease of the reorientational relaxation time between complete water coverage and solution, and on the fact that enzyme activity follows the same dependence (Rupley et al., 1983). The present results also suggest the evolution of the dynamic properties of the protein with hydration conditions where the thermodynamic properties do not change. Everything points to a situation where at 0.4 g/g (full hydration), all "solution" configurations were already accessible to the side chain residues, and where the contribution of further water molecules would only facilitate the diffusion between these configurations, therefore accelerating the motion and making it possible to explore a wider volume in a shorter time. If this is true, the heat capacity would not be directly affected, because the energy of each configuration would not be different at full hydration and in solution. Only the energy barriers between the different conformational substates (Frauenfelder et al., 1991) would be affected by hydration above full hydration, these energy barriers being lower in solution than at 0.4 g/g.

3. Dynamics for powders at 0.65 g/g, i.e., a hydration level higher than full hydration, is difficult to model because a certain amount of global diffusion probably appears to be too slow to be detected, but still rapid enough to prevent the interpretation of the internal motions. The existence of global motions in lysozyme-water systems at 0.5 g/g hydration has also been suggested by x-ray diffuse scattering measurements on tetragonal lysozyme crystals by Pérez et al. (1996). Thus considering the argumentation developed above for the effect of misfitting global motions in solutions, the amplitude and time-scale values of the real internal motions at 0.65 g/g should be between those of the 0.4 g/g powder and those of the solution.

An interesting point to be noted is that the value of $\langle u^2 \rangle$ derived from the Debye-Waller factor is almost insensitive to the level of hydration in powders. This is to be expected, because in our description, $\langle u^2 \rangle$ accounts only for the vibrational motions, which are a priori less influenced by the effect of hydration than the diffusive motions. We can note that the value obtained, $\sim$0.17 Å^2, is much lower, in the case of a hydrated powder, than that reported for $\langle u^2 \rangle$ by other authors at an ambient temperature, from incoherent elastic neutron scattering (Ferrand et al., 1993; Andreani et al., 1995) and Rayleigh scattering of Mössbauer radiation (Kurinov et al., 1987). But we must be careful about the fundamentally different meaning of the $\langle u^2 \rangle$ that these authors consider. In their approach, $\langle u^2 \rangle$ somehow accounts for both diffusive and vibrational motions and is deduced from a kind of generalized Debye-Waller factor, whereas our data analysis has the advantage of differentiating between diffusive and vibrational motions and allows the determination of a purely vibrational $\langle u^2 \rangle$. Bearing this in mind, we may easily reconcile our measurements of $\langle u^2 \rangle_{\text{vibr}}$ with the measurements of $\langle u^2 \rangle_{\text{total}}$ given in the literature. These studies show for $\langle u^2 \rangle_{\text{total}}$ a linear increase with temperature, typical of a harmonic behavior, independently of the hydration level and for temperatures below the dynamic transition, at $\sim$180K. A strong increase of $\langle u^2 \rangle_{\text{total}}$ above this transition is also observed, although only in the case of hydrated powders, because of the onset of diffusive motions. The numerical value obtained here for $\langle u^2 \rangle_{\text{vibr}}$, around 0.17 Å^2, is very close to the value extrapolated at room temperature from the harmonic behavior observed below the dynamic transition temperature of the generalized $\langle u^2 \rangle_{\text{total}}$, which is a very satisfactory result.

The comparison between the dynamics of lysozyme and myoglobin deserves a few comments. The main observation is that lysozyme appears to be more flexible at the picosecond time scale than myoglobin. More precisely, despite the proportion of diffusing nonexchangeable hydrogens, $(1 - p)$, being the same for the two proteins in solution, the amplitude of motions characterized by σ and the increase with Q of the internal quasielastic scattering are higher for lysozyme. One explanation could be that the number of hydrogens situated at the extremity of surface "flexible" side chains is proportionally higher in lysozyme. These hydrogen atoms are more susceptible than the others to experiencing large amplitude restrained diffusive motions. Table 2 shows the number of flexible residues with an accessible area higher than the 15 Å^2 of the most accessible carbon atoms. We considered as flexible those residues that contain at least one nonexchangeable hydrogen on a carbon atom at position δ or higher. Each accessible area was calculated with the program "surface" from the CCP4 suite

TABLE 2 Number of "extreme hydrogens," i.e., the nonexchangeable hydrogen atoms situated in surface residue side chains and bonded to a carbon atom situated at position δ or higher

	Lys		Arg		Ile		Leu		Phe		His		Trp		Total extreme H	Tot H
Lysozyme	6	24	8	16	2	6	1	6	1	5	0		1	5	62	696
Myoglobin	14	56	1	2	1	3	2	12	1	5	5	10	0		88	981

The two numbers given for each type of residue correspond to the number of such residues at the surface of the protein and to the associated number of extreme hydrogens. "Tot H" gives the total number of nonexchangeable hydrogen atoms in the protein.

of programs (1994) and represents the area of the locus of the center of a 1.4-Å-radius probe rolling on the surface of the protein. Table 2 also shows the number of nonexchangeable hydrogen atoms bonded to a carbon atom situated at position δ or higher (named "extreme hydrogens"). It is clear from the table that the ratio of extreme hydrogens to the total number of nonexchangeable hydrogens is slightly higher for myoglobin than for lysozyme.

This suggests a higher flexibility for myoglobin, contrary to what our IQENS results show. However, another source of lysozyme flexibility might come from the two-domain structure of this protein. In particular, the hinge-bending mode of hen egg white lysozyme has been evaluated from Langevin dynamics calculations by Wolynes and McCammon (1977), deriving an opening of the binding cleft by 1 Å, with a pseudoperiod of 20 ps (Brooks et al., 1988). Since then, dynamics calculations have concentrated more on the bacteriophage T4 lysozyme, for which the crystallographic confirmation of the existence of the bending mode was published (Faber and Matthews, 1990). Thus if we consider the above calculations, we immediately see that the hinge-bending mode may perfectly influence the protein internal dynamics considered in our experiment. The effect of such a mode would be to increase the hydrogen motion amplitude by ~1 Å and to enhance the diffusive character of this motion, exactly what is found in the present experiment.

CONCLUSION

The first aim of this work was to check the possibility of obtaining reliable data on the internal dynamics of proteins in solution by quasielastic neutron scattering. The main difficulty resided in the deconvolution of the scattering function due to global protein motions, which has been shown here to influence the contribution arising from internal motions. Although this type of deconvolution is usual in NMR spectroscopy, it has not been developed for neutron scattering. We suggest here a possible way to proceed to such a deconvolution. The present results have shown that from the same neutron scattering experiment, it is possible to obtain a global diffusion constant very much in agreement with classical measurements by quasielastic light scattering as well as internal dynamics parameters.

Besides this "technical" aspect of the work, our purpose, from a biological viewpoint, was to compare the dynamics of proteins in solution with that in hydrated powders. One of the basic known results in this aspect is that the protein heat capacity does not change upon hydration after complete coverage of the protein by water, which occurs at ~0.4 g/g for several globular proteins. However, this is not in opposition to a possible evolution of the internal dynamics, as suggested by the higher activity of many enzymes in solution compared to a completely hydrated powder. The interpretation proposed here is that from dry powder to complete coverage at 0.4 g/g, the surface side chains progressively acquire the possibility to diffuse locally, thanks to a few molecules of water that offer them several hydrogen-bonding pathways, and that on subsequent hydration, the main effect of water is to improve the rate of these diffuse motions, but without necessarily creating new hydrogen bonds. This might explain why the heat capacity does not change, whereas dynamics does. In particular, we have shown that motions with higher average amplitude occur in solution, about three times more than at 0.4 g/g, with a shorter average relaxation time, ~4.5 ps compared with 9.4 ps at 0.4 g/g.

Despite the use of two different models for the hydrogen motions, free diffusion in a sphere and three-site jump, we obtain the same results from the fitting of the experimental data. This suggests that the conclusions proposed here are model independent.

The last remark is that our technique is sensitive enough to differentiate between the dynamic behaviors of two proteins, because lysozyme appears to be more flexible than myoglobin. This point must be developed, in particular to check the influence of a many-domain structure on internal dynamics.

APPENDIX

We present here the equations and results of calculations concerning the effect on incoherent quasielastic neutron scattering of both translational and rotational diffusion of dense hard spheres in solution. All calculations were performed with IDL software.

The basic equations for either translational or rotational diffusion of a single, punctual, incoherent scatterer can be found in Bée (1988). The translational diffusion of a single particle is characterized by a diffusion constant, D_S. Incoherent scattering of a neutron by this particle produces a scattering function that is a Lorentzian in the ω-space,

$$S_{\text{trans}}(Q, \omega) = \frac{1}{\pi} \cdot \frac{\Gamma}{\omega^2 + \Gamma^2}, \quad \text{with } \Gamma = D_S Q^2 . \tag{A1}$$

The scattering function is the same for the translational diffusion of a dense hard sphere, because all scatterers within the sphere translate in the same way at the same time.

The isotropic rotational diffusion of a scatterer moving at the surface of a sphere of radius a is determined by a rotational diffusion constant D_{rot} and gives rise to a scattering function,

$$S_{\text{rot,single}}(Q, \omega) = \sum_{l=0}^{\infty} A_l(Q) \cdot \frac{1}{\pi} \cdot \frac{\tau_l}{1 + \omega^2 \tau_l^2}, \tag{A2}$$

with

$$A_l(Q) = (2l + 1) j_l^2(Qa) \quad \text{and} \quad \tau_l = \frac{1}{l(l + 1) D_{\text{rot}}}, \tag{A3}$$

and where the $j_l(x)$ are spherical Bessel functions. At a given Q, $S_{\text{rot}}(Q, \omega)$ is an infinite sum of normalized Lorentzians with increasing width, each weighted by a factor $A_l(Q)$. Note that τ_l in Eq. A2 depend only on D_{rot}, and $A_l(Q)$ only on the radius of rotation. To model the isotropic rotational diffusion of a dense hard sphere, we must consider the rotational diffusion of each infinitesimal volume within the sphere. As we are dealing with incoherent scattering, each infinitesimal volume at a distance r from the sphere center produces a scattering function given by Eq. A2, in which a is replaced by r in Eq. A3. Then we have to integrate this function over the

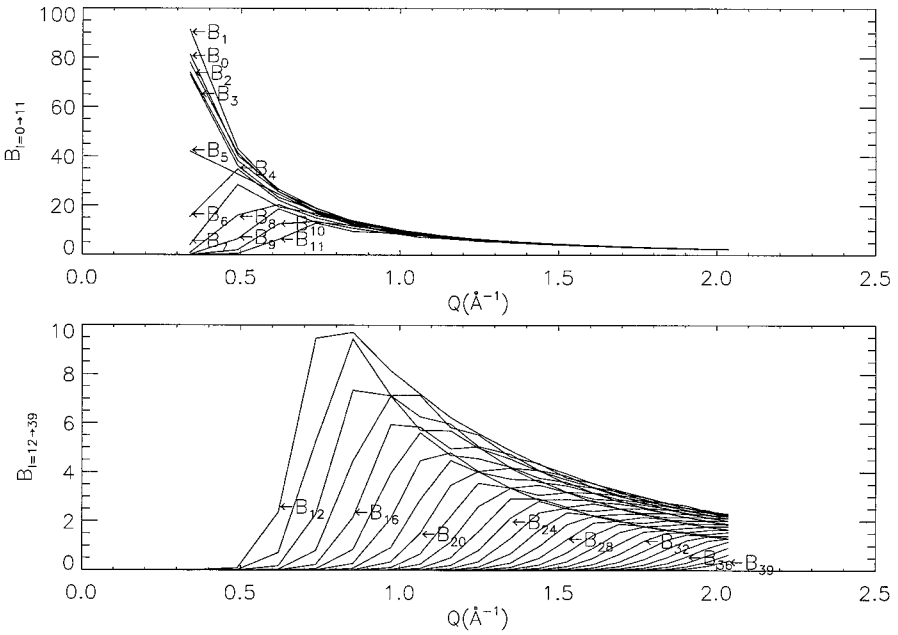

FIGURE 8 Plot of the first 39 terms of Eq. A5. The number of useful terms depends on the maximum value of Q one is interested in and increases with R. For R = 19 Å, and Q_{max} = 2 Å^{-1}, 39 terms are necessary.

volume of the sphere to get the total scattering function,

$$S_{\text{rot,dense sphere}}(Q, \omega) = \sum_{l=0}^{\infty} B_l(Q) \cdot \frac{1}{\pi} \cdot \frac{\tau_l}{1 + \omega^2 \tau_l^2}, \qquad \text{(A4)}$$

with

$$B_l(Q) = \int_{r=0}^{R} A_{l,r}(Q) \cdot 4\pi \cdot r^2 \mathrm{d}r$$

and

$$A_{l,r}(Q) = (2l + 1) j_l^2(Qr) \qquad \text{(A5)}$$

Fig. 8 shows a plot of the first 39 $B_l(Q)$ for a dense hard sphere of radius R = 19 Å. The B_l were calculated for each experimental value of Q by numerical integration. The number of terms necessary to obtain convergence in the theoretically infinite sum in Eq. A4 depends on the maximum value of Q one wants to cover and increases as the radius of the sphere increases. It is clear from the figure that 39 terms are enough for Q_{max} = 2 Å^{-1} with R = 19 Å.

The combination of independent translational and rotational motions of a dense hard sphere implies the convolution of the respective scattering functions; thus

$$S_{\text{trans\&rot}}(Q, \omega) = \sum_{l=0}^{39} B_l(Q) \cdot \frac{1}{\pi} \cdot \frac{\left(\Gamma(Q) + \frac{1}{\tau_l}\right)}{\omega^2 + \left(\Gamma(Q) + \frac{1}{\tau_l}\right)^2}, \qquad \text{(A6)}$$

As a test, the function $S_{\text{trans\&rot}}(Q, \omega)$ was plotted for the experimental values of Q as a function of ω with R = 19 Å, the hydrodynamic radius of lysozyme. We used the value of D_S expected for lysozyme from the Einstein relation at 20°C (see the Data Analysis section), i.e., $D_S = 6.1 \times 10^{-3}$ meVÅ^2, and the corresponding value of D_{rot}, according to $D_{rot} = 3 \cdot D_S/(4 \cdot R^2)$. The functions obtained are plotted as a function of ω in Fig. 9, for two values of Q. It is clear that these functions are perfectly approximated by Lorentzians. Fig. 10 shows the variation with Q of $\Gamma_{\text{trans\&rot}}$, the

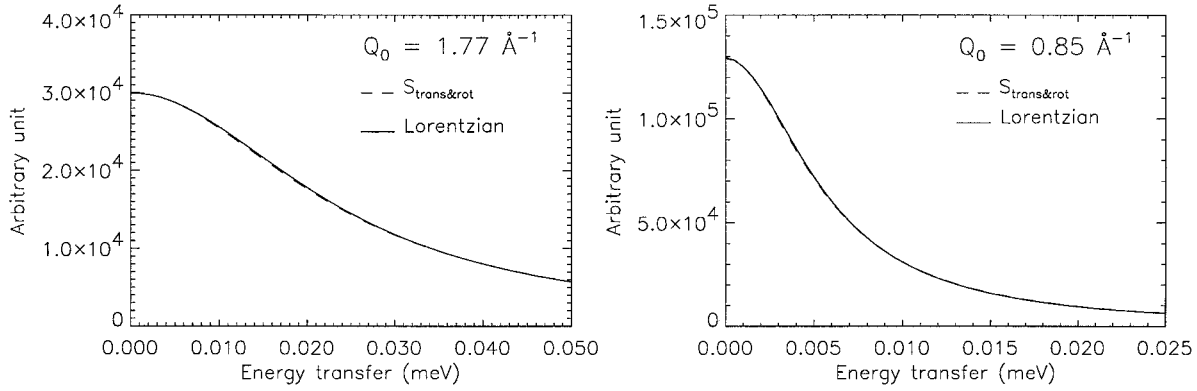

FIGURE 9 Comparison between the calculated scattering function $S_{\text{trans\&rot}}(Q, \omega)$ and a Lorentzian function at two different values of Q. The curves can be superimposed. $S_{\text{trans\&rot}}(Q, \omega)$ was calculated with R = 19 Å, $D_S = 6.1 \times 10^{-3}$ meV · Å^2, and $D_{rot} = 3 \cdot D_S/(4 \cdot R^2)$.

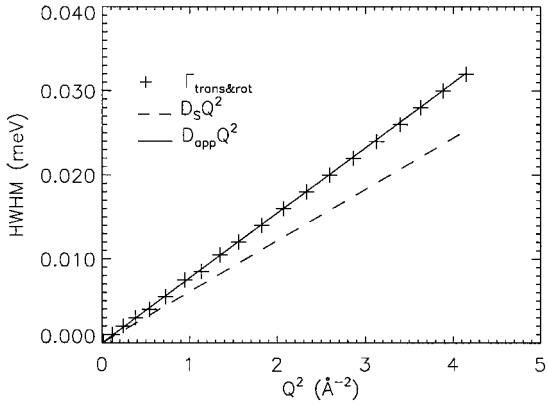

FIGURE 10 Half-width at half-maximum, Γ_{sph}, of $S_{trans\&rot}(Q, \omega)$ as a function of Q (*crosses*). The variation of Γ_{sph} is quadratic in Q, following the classical diffusion law, $\Gamma_{sph} = D_{app}Q^2$, with D_{app} higher than D_S by ~27%. The law for purely translational diffusion, D_SQ^2, is also plotted, as a reference.

HWHM of $S_{trans\&rot}(Q, \omega)$. $\Gamma_{trans\&rot}$ follows the law $\Gamma = D_{app}Q^2$, with D_{app} higher than D_S by ~27%. In conclusion, the effect of the rotational motions only modifies the apparent value of the diffusion constant, and the translational diffusion law can be kept as the model to use in the fitting procedure for global motions.

We thank José Dianoux (Institut Laue-Langevin, Grenoble) for his assistance as a local contact during the IN6 experiment, Don Curley and Marc Bée (ILL) for very helpful software, and Didier Lairez (LLB, Saclay) for performing the QELS experiments. We also thank Marie-Claire Bellissent-Funel (LLB) and José Teixeira (LLB) for useful discussions.

REFERENCES

Andreani, C., A. Filabozzi, F. Menzinger, A. Desideri, A. Deriu, and D. Di Cola. 1995. Dynamics of hydrogen atoms in superoxide dismutase by quasielastic neutron scattering. *Biophys. J.* 68:2519–2523.

Bée, M. 1988. Quasielastic Neutron Scattering. Principles and Applications in Solid State Chemistry, Biology and Materials Science. Adam Hilger, Bristol and Philadelphia.

Bellissent-Funel, M. C., J.-M. Zanotti, and S. H. Chen. 1996. Slow dynamics of water molecules on the surface of a globular protein. *Faraday Discuss.* 103:281–294.

Brooks, C. L., III, M. Karplus, and B. M. Pettitt. 1988. Proteins: A Theoretical Perspective of Dynamics, Structure, and Thermodynamics. John Wiley and Sons, New York.

Cantor, C. R., and P. R. Schimmel. 1980. Biophysical Chemistry. Part II: Techniques for the Study of Biological Structure and Function. Freeman & Co., San Francisco. 570–588.

Carpentier, L., M. Bée, A. M. Giroud-Godquin, P. Maldivi, and J. C. Marchon. 1989. Alkyl chain motions in columnar mesophases. A quasielastic neutron scattering study of dicopper tetrapalmitate. *Mol. Phys.* 68:1367–1378.

Collaborative Computational Project, Number 4. 1994. The CCP4 suite: programs for protein crystallography. *Acta Crystallogr.* D50:760–763.

Denisov, V. P., and B. Halle. 1995. Protein hydration dynamics in aqueous solution: a comparison of bovine pancreatic trypsin inhibitor and ubiquitin by oxygen-17 spin relaxation dispersion. *J. Mol. Biol.* 245: 682–697.

Diehl, M., W. Doster, W. Petry, and H. Schober. 1997. Water-coupled low-frequency modes of myoglobin and lysozyme observed by inelastic neutron scattering. *Biophys. J.* 73:2726–2732.

Doster, W., S. Cusack, and W. Petry. 1989. Dynamical transition of myoglobin revealed by inelastic neutron scattering. *Nature.* 337: 754–756.

Drapron, R. 1985. Properties of water in foods in relation to quality and stability. *NATO Adv. Study Inst. Ser. E.* 90:171–190.

Faber, H. R., and B. W. Matthews. 1990. A mutant T4 lysozyme displays five different crystal conformations. *Nature.* 348:263–266.

Ferrand, M., A. J. Dianoux, W. Petry, and G. Zaccaï. 1993. Thermal motions and function of bacteriorhodopsin in purple membranes: effects of temperature and hydration studied by neutron scattering. *Proc. Natl. Acad. Sci. USA.* 90:9668–9672.

Fitter, J., R. E. Lechner, G. Büldt, and N. A. Dencher. 1996. Internal molecular motions of bacteriorhodopsin: hydration-induced flexibility studied by quasielastic incoherent neutron scattering using oriented purple membranes. *Proc. Natl. Acad. Sci. USA.* 93:7600–7605.

Fitter, J., R. E. Lechner, and N. A. Dencher. 1997. Picosecond molecular motions in bacteriorhodopsin from neutron scattering. *Biophys. J.* 73: 2126–2137.

Frauenfelder, H., S. G. Sligar, and P. G. Wolynes. 1991. The energy landscapes and motions of proteins. *Science.* 254:1598–1603.

Goldanskii, V. I., and Y. F. Krupyanskii. 1989. Protein and protein-bound water dynamics studied by Rayleigh scattering of Mössbauer radiation (RSMR). *Q. Rev. Biophys.* 22:39–92.

Gregory, R. B. 1995. Protein-Solvent Interactions. Marcel Dekker, New York.

Gregory, R. B., and K. J. Chai. 1993. 4th International Workshop on Positron and Positronium Chemistry. *J. Physique IV.* 3:305–310.

Jacrot, B. 1976. The study of biological structures by neutron scattering from solution. *Rep. Prog. Phys.* 39:911–953.

Knapp, E. W., S. F. Fischer, and F. Parak. 1982. Protein dynamics from Mössbauer spectra. The temperature dependence. *J. Phys. Chem.* 86: 5042–5047.

Kneller, G. R., and J. C. Smith. 1994. Liquid-like side-chain dynamics in myoglobin. *J. Mol. Biol.* 242:181–185.

Kuehner, D. E., C. Heyer, C. Ramsch, U. M. Fornefeld, H. W. Blanch, and J. M. Prausnitz. 1997. Interactions of lysozyme in concentrated electrolyte solutions from dynamic light-scattering measurements. *Biophys. J.* 73:3211–3224.

Kuntz, I. D., Jr., and W. Kauzmann. 1974. Hydration of proteins and polypeptides. *Adv. Protein Chem.* 28:239–345.

Kurinov, I. V., Yu. F. Krupianskii, I. P. Suzdalev, and V. I. Goldanskii. 1987. RSMR study of the hydration effect on the dynamics of some globular proteins. *Hyperfine Interactions.* 33:223–232.

Lechner, R. E., N. A. Dencher, J. Fitter, G. Bueldt, and A. V. Belushkin. 1994a. Proton diffusion on purple membrane studied by neutron scattering. *Biophys. Chem.* 49:91–99.

Lechner, R. E., N. A. Dencher, J. Fitter, and Th. Dippel. 1994b. Two-dimensional proton diffusion on purple membrane. *Solid State Ionics.* 70/71:296–304.

McCammon, J. A., and S. C. Harvey. 1987. Dynamics of Proteins and Nucleic Acids. Cambridge University Press, New York.

Millero, F. J., R. Dexter, and E. Hoff. 1971. Density and viscosity of deuterium oxide solutions from 5–70°C. *J. Chem. Eng. Data.* 16:85–87.

Pérez, J., Ph. Faure, and J. P. Benoit. 1996. Molecular rigid-body displacements in tetragonal lysozyme crystal confirmed by x-ray diffuse scattering. *Acta. Crystallogr.* D52:722–729.

Rasmussen, B. F., A. M. Stock, D. Ringe, and G. A. Petsko. 1992. Crystalline ribonuclease A loses function below the dynamical transition at 200 K. *Nature.* 357:423–424.

Receveur, V., P. Calmettes, J. C. Smith, M. Desmadril, G. Coddens, and D. Durand. 1997. Picosecond dynamical changes on denaturation of yeast phosphoglycerate kinase revealed by quasielastic neutron scattering. *Proteins.* 28:380–387.

Riès-Kautt, M., and A. Ducruix. 1997. Inferences drawn from physicochemical studies of crystallogenesis and precrystalline state. *Methods Enzymol.* 276:23–59.

Rupley, J. A., and G. Careri. 1991. Protein hydration and function. *Adv. Protein Chem.* 41:37–172.

Rupley, J. A., E. Gratten, and G. Careri. 1983. Water and globular proteins. *Trends Biochem. Sci.* 8:18–22.

Rupley, J. A., P. H. Yang, and G. Tollin. 1980. Water in Polymers. ACS Symposium Series, Vol. 127. S. P. Rowland, editor. American Chemical Society, Washington, DC. 111–132.

Settles, M., and W. Doster. 1996. Anomalous diffusion of adsorbed water: a neutron scattering study of hydrated myoglobin. *Faraday Discuss.* 103:1–10.

Smith, J. C. 1991. Protein dynamics: comparison of simulations with inelastic neutron scattering experiments. *Q. Rev. Biophys.* 24:1–65.

Van Hove, L. 1954. Correlations in space and time and Born approximation scattering in systems of interacting particles. *Phys. Rev.* 95: 249–262.

Venkatesan, M., C. S. Hirtzel, and R. Rajagopalan. 1985. The effect of colloidal forces on the self-diffusion coefficients in strongly interacting dispersions. *J. Chem. Phys.* 82:5685–5695.

Volino, F., and A. J. Dianoux. 1980. Neutron incoherent scattering law for diffusion in a potential of spherical symmetry: general formalism and application to diffusion inside a sphere. *Mol. Phys.* 41:271–279.

Walters, R. R., J. F. Graham, R. M. Moore, and D. J. Anderson. 1984. Protein diffusion coefficient measurements by laminar flow analysis: method and applications. *Anal. Biochem.* 140:190–195.

Weast, R. C. 1974. Handbook of Chemistry and Physics. CRC Press, Cleveland. F49.

Wolynes, P. G., and J. A. McCammon. 1977. Hydrodynamic effect on coagulation of porous biopolymers. *Macromolecules.* 10:86–87.

Yang, P., and J. A. Rupley. 1979. Water and globular proteins. *Biochemistry.* 18:2654–2661.

Zanotti, J.-M., M.-C. Bellissent-Funel, and J. Parello. 1997. Dynamics of a globular protein studied by neutron scattering and solid-state NMR. *Physica B.* 234–236:228–230.